Component-based Modelling of EV Battery Chargers

Component-Based Modelling of EV Battery Chargers

Xu Xiao, He Molin, Paraskevi Kourtza,
Adam Collin, Gareth Harrison and Sasa Djokic
The University of Edinburgh
Edinburgh, Scotland, UK

Jan Meyer, Sascha Müller, Friedemann Möller
Technische Universitaet Dresden
Dresden, Germany

***Abstract*—This paper reviews typical circuit topologies and control algorithms for on-board unidirectional single-phase electric vehicle battery chargers (EVBCs) and provides simple yet reasonably accurate component-based models for their representation for power system analysis. The accuracy of the developed models is validated against measurements of actual EVBCs, for both ideal voltage supply conditions and typically distorted voltage supply waveforms. The paper also provides exponential and polynomial EVBC model interpretations, as well as some discussion of the further use of the presented models for the analysis of existing networks and future smart grids with high penetration levels of EVBCs.**

***Index Terms*—Active power factor control, electric vehicle battery chargers, load modelling, power system analysis.**

I. INTRODUCTION

Electric vehicles (EVs) are recognised as one of the most promising technologies to help reduce the fossil fuel dependency in the road transportation sector. However, the connection of a large number of EV battery chargers (EVBCs) will present a major challenge for the operation of existing distribution networks, as these loads might cause significant changes in power flows, with an inherent impact on voltage profiles, harmonic emissions and overall system performance. Currently, these changes are not fully understood. For example, a study in [1] suggested that uncontrolled charging of EVs with a relatively low (10%) penetration might increase peak demands by up to 18%. On the other hand, study in [2] suggested that connection of a number of different types of EVBCs could result in significant harmonic cancelation, which is beneficial to the distribution network operation.

To study the extent and range of these changes, in terms of impact on power flows and power quality, correct models of EVBCs are required. Depending on the type of charger and purpose of modelling, a variety of component-based EVBC models have been described in existing literature (with a broad summary in [3]). However, simplified models suitable for a large area network studies are still not widely available, as most of existing literature (e.g. [4], [5]) focuses on the design of EVBCs, presenting models which generally could not represent the electrical characteristics of existing commercial EVBCs. This paper addresses the above issues and presents component-based models of single-phase unidirectional on-board EVBCs, which are representative of those available on the EU domestic market and are capable of reproducing relevant electrical characteristics with a reasonable accuracy.

The authors acknowledge support by the German Federal Ministry for the Environment, Nature Conservation, Building and Nuclear Safety (project ElmoNetQ, FKZ: 16EM1052).

The research presented in this paper continues the EVBC modelling work presented in [6], aimed at producing simple yet accurate models for analysing the effects of increased penetration of EVs on low voltage (LV) and medium voltage (MV) networks. The capability of the presented models to correctly represent both steady-state and harmonic power flow characteristics of the modelled EVBCs is validated against available measurements.

II. TYPICAL EVBC CIRCUITS AND CONTROLS

The battery charger is an important component of the EV, as it has direct impact on battery life and required charging times, modes and conditions. There are several possible variants of EVBCs, with classification based on: charging voltage and current (single-phase, three-phase, or dc), charger location (on-board, or off-board) and power flow direction (unidirectional, or bidirectional).

The requirements for EVBC performance vary depending on EV application and have significant impact on EVBC's input characteristics, with [7] and [8] specifying limits for the single-phase unidirectional on-board chargers considered in this paper. As EVBCs are a relatively new type of load, there is still no specification of dedicated harmonic limits in [7], which instead recommends the requirements for Class A equipment from [8]. Accordingly, EVBCs will typically have an active power factor control (a-PFC) circuit, to limit their harmonic emissions and reactive power demands. However, if the input ac supply voltage waveform is distorted, as is typically true in LV residential networks, the control of the a-PFC circuit will not be able to produce the desired ideally sinusoidal input ac current [9]. This clearly indicates that the correct modelling of EVBCs should include a-PFC circuit.

A. Full Circuit EVBC Model

The EVBC is a complex power electronic circuit, with main components illustrated in Fig. 1. The key functional blocks are described in the subsequent text, with the full circuit model presented overleaf in Fig. 2.

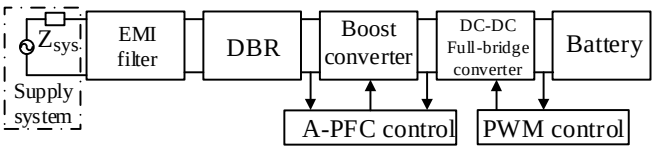

Figure 1. Main components of a single-phase unidirectional EVBC.

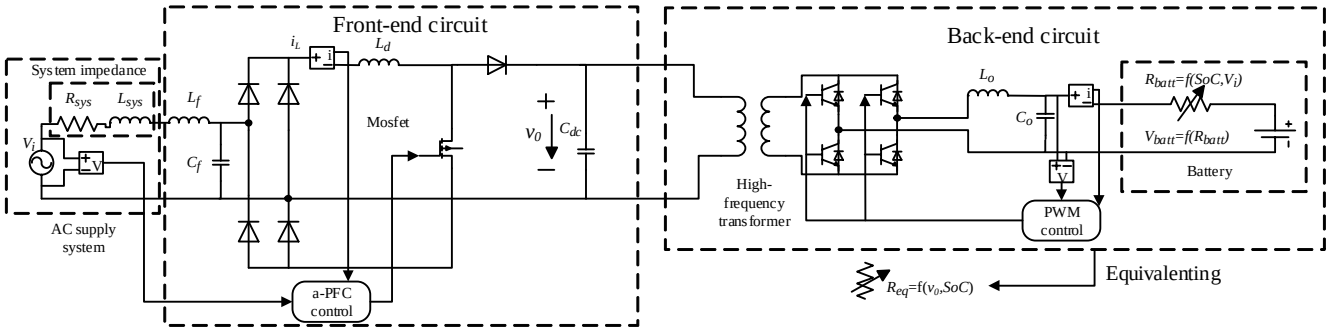

Figure 2. Full circuit model of a single-phase unidirectional EVBC circuit.

Before the boost converter, typical EVBC circuits have standard diode bridge rectifier (DBR) and input filter, as shown on the left-hand side of Fig. 2. Their main functions are: to rectify input ac voltage to dc, and to filter the high-frequency harmonics of input current. The EVBC front-end circuit could use a number of converter topologies, e.g. boost, buck, buck-boost, cúk, flyback or forward. However, the most widely used a-PFC topology is a boost converter with inductor current kept in a continuous conduction mode [3, 10], which is implemented in the EVBC models presented in this paper.

1) Front-end DC-DC Boost Converter and a-PFC Control: There are a variety of a-PFC control techniques, including average or peak current control and fixed-band or sinusoidal hysteresis current control. They typically consist of an outer voltage loop and an inner current loop control, where the value for the reference inductor current in the inner current loop is given by the amplified dc voltage error in the outer voltage loop, with the aim to maintain dc-side voltage at a desired value. The current control keeps inductor current (and hence input ac current) within the defined upper and lower boundary, while the control of the switching of the front-end converter is reconstructing the sinusoidal waveform, with either fixed or variable switching rate of inductor's current.

The a-PFC circuit from the developed full circuit EVBC model is shown in Fig. 3. Unlike traditional current control circuit, in which reference input current is obtained from the amplified dc-link voltage error, the applied modified peak current control neglects the voltage loop and sets the reference magnitude of input current directly in the current control loop, in order to better fit the measured data. The used control circuit is based on a conventional peak current control, with an added lower boundary for inductor current. The inductor current is first compared with its lower boundary, and boost converter is switched on if current is lower than its boundary value, resulting in an increase of the inductor current. When inductor current is above its lower boundary, the difference between the inductor current and its upper boundary is compared with a ramp signal to generate pulse width modulation (PWM) control for the boost converter switch. The frequency of the ramp signal is set at 35.8 kHz, which is also the switching frequency of the boost converter in the front-end circuit of a measured EV charger.

Fig. 4 illustrates the results for the applied modified peak current control circuit, showing that it can better model the input ac current waveform characteristics, i.e. its total harmonic distortion (THD_i) and harmonic magnitudes/phase angles, than the other three considered a-PFC control circuits.

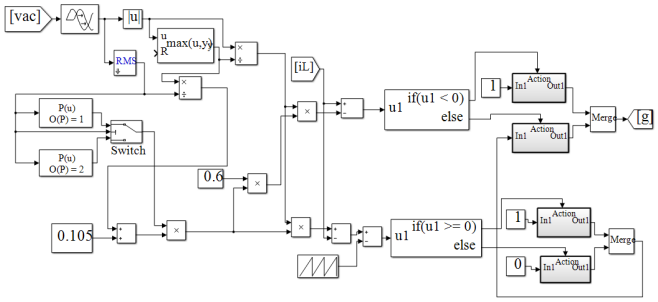

Figure 3. The developed a-PFC control circuit.

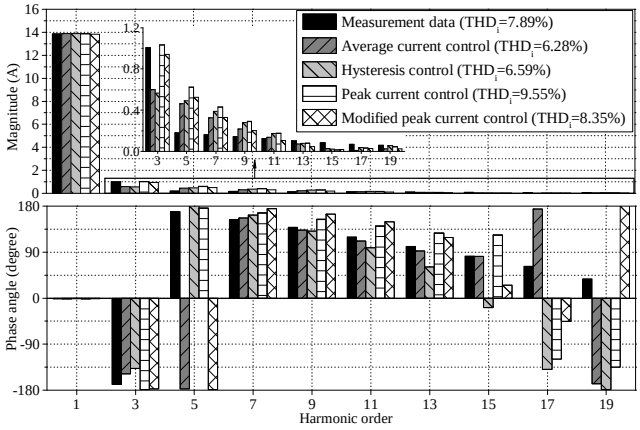

Figure 4. Comparison of input ac current harmonic magnitudes, phase angle and THD values between measurements and considered a-PFC circuits.

2) High-frequency transformer: In the EVBC circuit, a high-frequency transformer is typically (but not always) used for galvanic isolation, safety and better control of the voltages supplied to the battery by the back-end converter circuit.

3) Back-end DC-DC Full-bridge Converter with Battery Charging Control: The back-end dc-dc full-bridge converter is operated as a part of a battery management unit, to regulate battery charging in two general modes: constant current (CC) and constant voltage (CV). Initially, the battery current is

kept constant at the reference value (CC mode). When battery voltage reaches its reference value, it is kept constant (CV mode). From testing of EVs, it is found that the CC charging mode is active up to around 80%-90% of battery's full state of charge and that its duration is much longer than the CV mode, which typically lasts only a few to several tens of minutes (and sometimes even less than that).

The control circuit of the full-bridge converter in the developed EVBC model is shown in Fig. 5. The reference values for battery current and voltage are set at 6.5A and 360V respectively, which is derived from the actual measurement data, as shown in Fig. 6. The PWM signal for controlling the switching of the transistors is generated by comparing the amplified voltage or current error with a ramp signal, with the same switching frequency as the front-end boost converter.

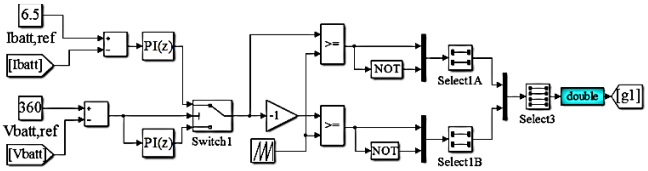

Figure 5. The control circuit of the dc-dc full-bridge converter.

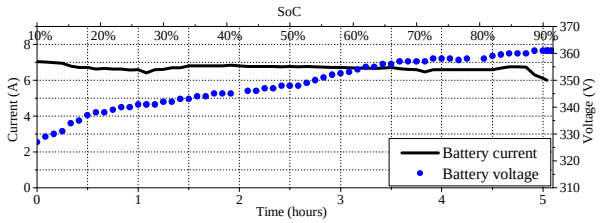

Figure 6. Measured battery voltage and current for EVBC charging under 1pu sinusoidal input ac voltage.

4) Battery: Although the EV battery (typically Li-ion type) is not an actual component of the EVBC, accurate representation of the battery is important for the correct EVBC modelling. The battery resistance in the presented model is expressed as a function of battery charging time (i.e. SoC) and rms value of the input ac voltage magnitude (i.e. V_i), where the relationship between battery resistance and battery charging time is determined from measurements of the EV battery and found to be approximately linear, Fig. 7.

The battery equivalent resistance decreases with reducing ac supply voltage magnitude, which is described by the following relationship:

$$R_{batt}\begin{cases} 6.47SoC + 60.66V_i - 9.84, & 0.80 \le V_{i,pu} \le 1.0 \\ 6.47SoC - 48.39V_i^2 + 112.12V_i - 14.84 & 1.0 < V_{i,pu} \le 1.20 \end{cases} \quad (1)$$

The reason for two operation regions in (1) is that R_{batt} will increase much more slowly when V_i is above 0.95pu than when V_i is at or below 0.95pu. For the tested EVBC, this is clearly illustrated in Fig. 13a, which shows a change in the EVBC power demand characteristic from a constant current load type to a constant power load type when V_i is higher than around 0.95pu-1pu. Consequently, when battery is charged in CC mode, R_{batt} should increase linearly with V_i, for V_i values below 0.95pu-1pu, while above this value (assuming constant power conversion efficiencies for different V_i values), R_{batt} will remain approximately constant in the model. This is validated in Fig. 7, which shows that V_i values above 0.95pu-1pu have only a small impact on the battery resistance.

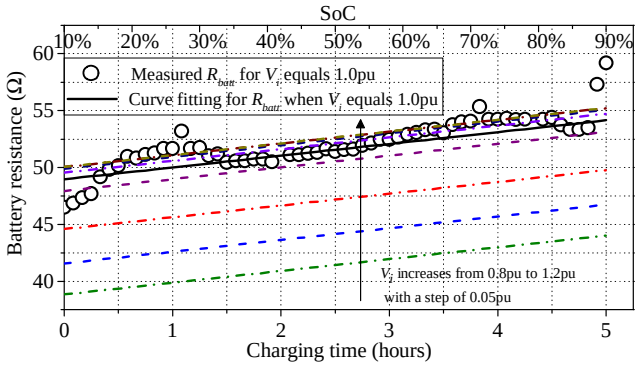

Figure 7. Measured battery resistance during CC charging mode.

B. *Equivalent Circuit EVBC Model*

The full circuit EVBC model is very accurate, but requires modelling of relatively complex electronic circuits, resulting in high computational/modelling requirements and excessively long simulation times. In order to resolve these issues, the high-frequency transformer, full bridge converter and battery are replaced by an analytical expression for the equivalent time-variable resistance, R_{eq}, as shown in Fig. 2.

The relationship for R_{eq} is calculated from the instantaneous dc-link current and dc-link voltage and this process is repeated across the extended range of input ac voltages (from 0.8pu to 1.2pu). This is displayed in Fig. 8, which shows that the R_{eq} is increasing almost linearly with an increase of the instantaneous dc-link voltage, v_0. The general equation for R_{eq} is written as (2), which is obtained after a detailed analysis and fitting of model parameters to the values measured in tests with actual EVBCs.

$$R_{eq} = (0.013SoC + 0.117)v_0 + 0.216SoC^2 + 0.0845SoC + 0.268 \quad (2)$$

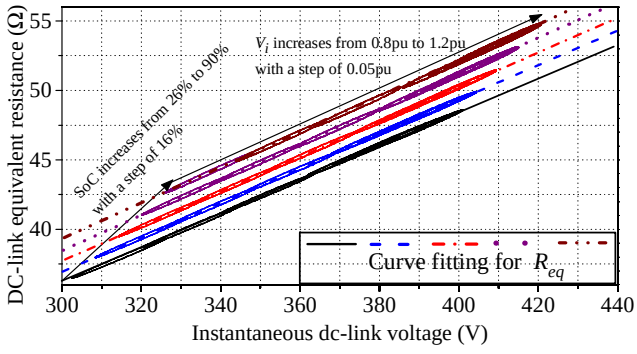

Figure 8. The relationship between the equivalent resistance (R_{eq}) and dc-link voltage (v_0) under 0.8pu - 1.2pu sinusoidal input ac voltage.

III. VALIDATION OF THE DEVELOPED EVBC MODELS

To validate the developed EVBC models, a commercially available single-phase on-board EVBC was connected to a controllable power source and subjected to a number of tests.

The main criteria for the validation was ability of the EVBC models to reproduce the measured input ac current waveforms for a range of input ac supply voltage conditions and source impedances. The three characteristic supply voltage waveforms applied in the tests are shown in Fig.9, while only results for zero source impedance are given in this paper.

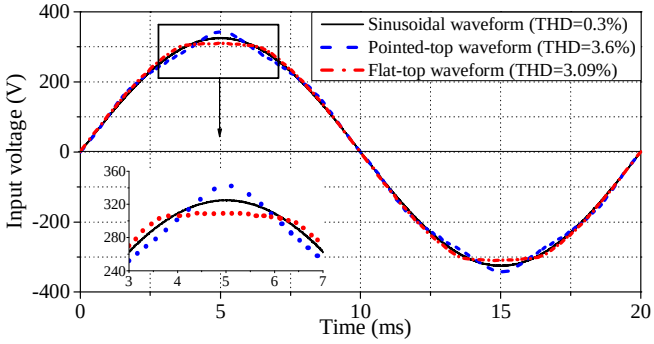

Figure 9. The three characteristic waveforms used in tests.

Comparisons of simulation and measurement results for 1pu ideally sinusoidal, 'pointed-top' and 'flat-top' input ac voltage waveforms are shown in Fig. 10, 11 and 12, respectively. Fig. 13 provides further validation of the developed EVBC models, with respect to their capability to reproduce voltage-dependent electrical characteristics. While measurement data were available for 0.8pu-1.1pu range of input ac voltages, simulation data are obtained for the range of 0.8pu-1.2pu, in order to better quantify the EVBC behaviour.

A. Ideally Sinusoidal Input AC Supply Voltage Waveform

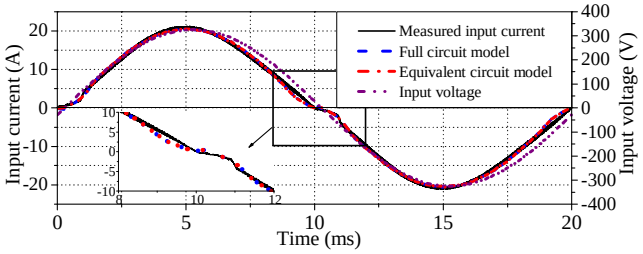

a) instantaneous input ac current waveforms

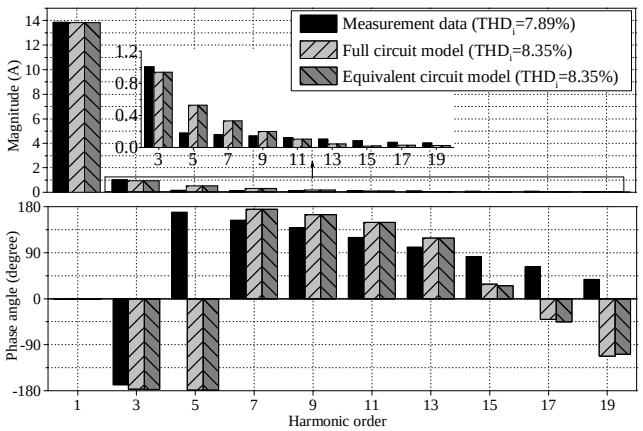

b) input current harmonics

Figure 10. Comparison of measured and simulated input ac currents for 1 pu ideally sinusoidal input ac supply voltage.

B. Distorted Input AC Supply Voltage Waveform

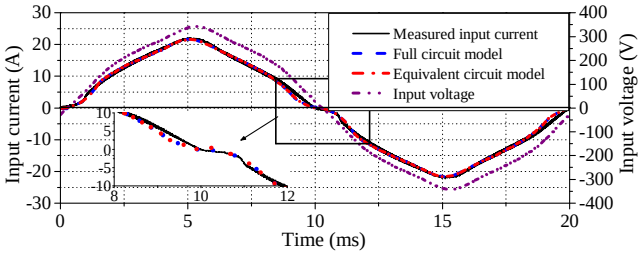

a) instantaneous input ac current waveforms

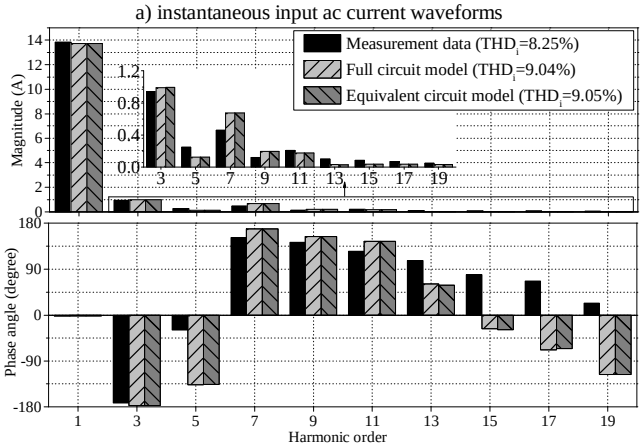

b) input current harmonics

Figure 11. Comparison of measured and simulated input ac currents for 1 pu "pointed-top" input ac supply voltage.

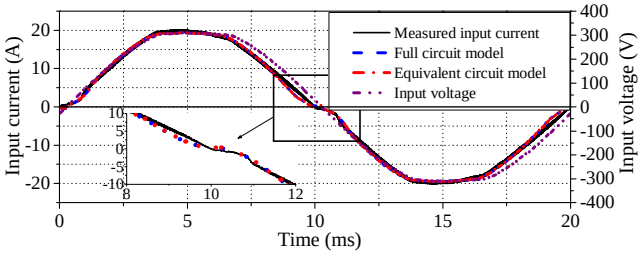

a) instantaneous input ac current waveforms

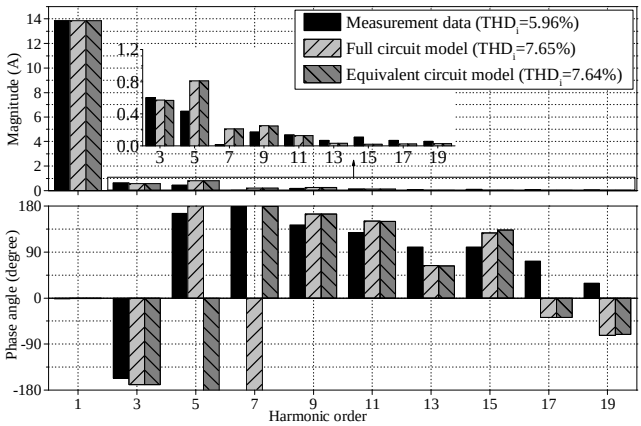

b) input current harmonics

Figure 12. Comparison of measured and simulated input ac currents for 1pu "flat-top" distorted input ac supply voltage.

C. Comparison of Electrical Load Characteristics

Figure 13 compares electrical characteristics derived from measurement and simulation data for the considered range of input ac voltages (0.8pu-1.2pu). The electrical characteristics are represented by plotting dependencies of active power, P, fundamental reactive power, Q_1, and total current harmonic distortion, THD_i, as well as true, displacement and distortion power factors (PF, PF_1 and PF_d, respectively) on ac supply voltage magnitude (for ideally sinusoidal waveforms). All calculations are performed in accordance to definitions in [11].

It can be seen from Fig. 13 that the EVBC models can reproduce the relevant electrical characteristics of the tested EVBC with a reasonable accuracy. A somewhat higher error between the measured and simulated THD_i values is due to the corresponding differences in the calculated values of the 5th and 7th input ac current harmonic magnitude. Due to the low THD_i values, however, the absolute error is small.

The P-V and Q_1-V characteristics in Figs. 13a and 13b are of particular interest for modelling EVBCs in network studies. Fig. 13a shows that the modelled EVBC will change its active power demand characteristics from (an approximately) constant current load type to (an approximately) constant power load type for $V_i > 0.95$pu. The Q_1-V characteristic in Fig. 13b (normalized using Q_1 at nominal voltage) are similar, with a change from an approximately constant impedance load type to an approximately constant current type for $V_i > 0.95$pu. This is discussed further in the next section.

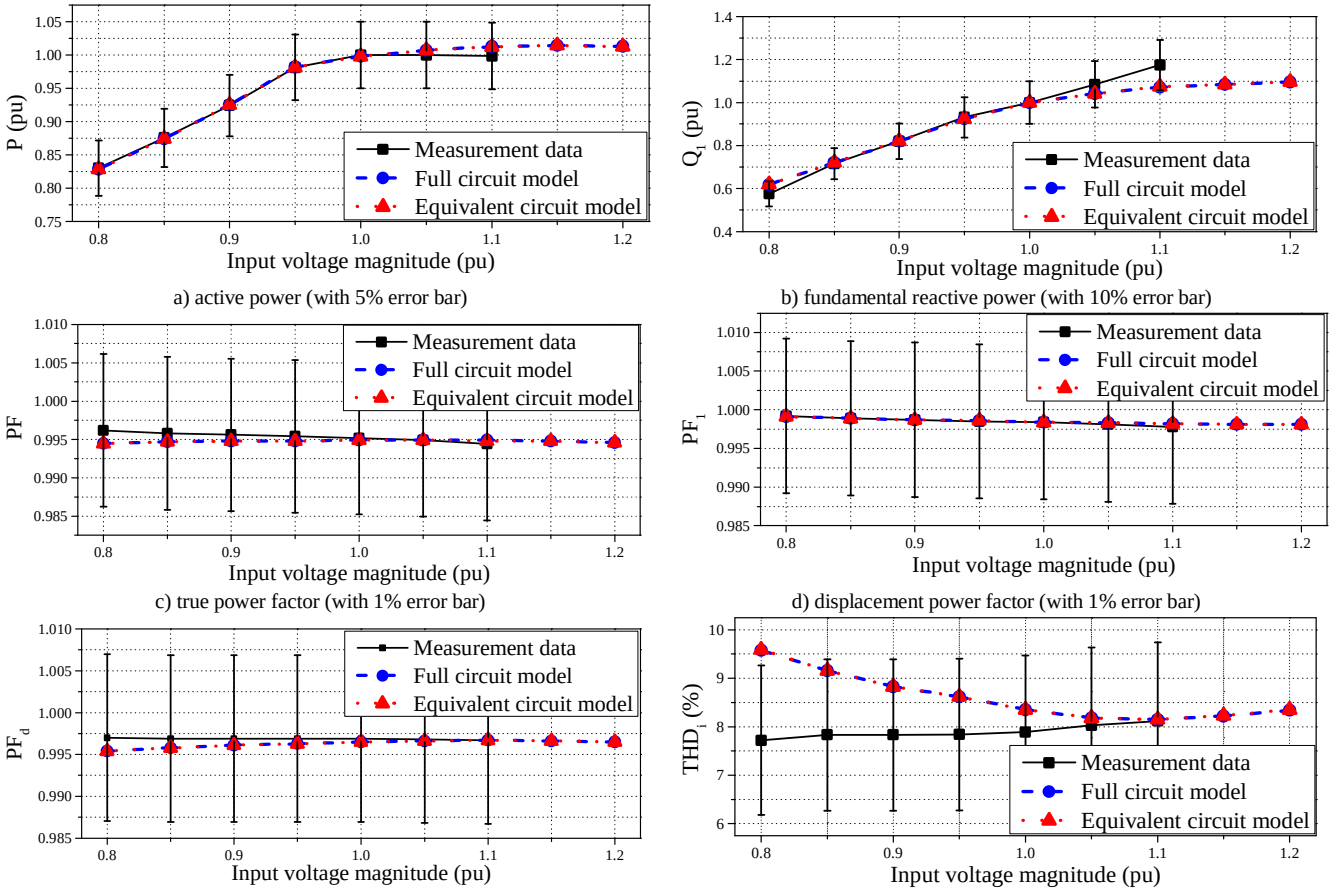

Figure 13. Comparison of selected electrical characteristics derived from measurement and simulation data (for 0.8 pu to 1.2 pu sinusoidal input voltages).

IV. Discussion of Network Model Applications

The presented equivalent circuit EVBC model (Table I) can be applied directly in network studies, or as a part of an iterative time and/or frequency domain modelling approach.

TABLE I. Parameter Values of the EVBC Model.

L_f (mH)	C_f (μF)	L_d (mH)	C_{dc} (μF)	Transformer R_1,R_2	Transformer L_1, L_2	Lo (mH)	Co (μF)	ramp signal f_s (kHz)	ramp signal output value
1.00 E-01	1.00 E-03	1.10 E+01	1.30 E+03	3.376	0.358	1.00 E+01	1.00 E+02	35.8	[0 3]

Standard steady state load model forms, i.e. exponential or ZIP models (Table II), can be extracted from the presented EVBC models due to their ability to reproduce voltage-dependent power demand characteristics. This allows the presented models to be used in most, if not all commercial power flow software packages to analyse LV/MV networks. For example, voltage dependency of active and reactive power demands is particularly important for assessing the EVBC potential for conservation voltage reduction in future networks with large penetration levels of EVs, as well as for the general assessment of network voltage profiles and power flows.

TABLE II. EXPONENTIAL AND ZIP EVBC MODEL INTERPRETATIONS.

Supply	PF_1	Exp. model		Polynomial/ZIP model					
		n_p	n_q	Z_p	I_p	P_p	Z_q	I_q	P_q
Ideal (<1pu)	0.998	0.88	2	0	0.89	0.11	1	0	0
PT (<1pu)	0.999	0.89	2	0	0.9	0.1	1	0	0
FT (<1pu)	0.995	0.89	2	0	0.9	0.1	1	0	0
Ideal (≥1pu)	0.998	0.08	0.46	0	0.08	0.92	0	0.47	0.53
PT (≥1pu)	0.999	0.03	0	0.01	0.02	0.97	0	0	1
FT (≥1pu)	0.995	0.07	0.51	0	0.07	0.93	0	0.51	0.49
where: Ideal – sinusoidal, PT – pointed-top, and FT – flat-top waveform.									

Model parameters for active power demand characteristics in Table II demonstrate that the EVBC will shift from an approximately constant current load type (with n_p~0.9 and I_p dominant in ZIP model) to an approximately constant power load type (i.e. with n_p~0 and P_p dominant in ZIP model) when input ac voltage magnitude is higher than 1pu. This is a consequence of the discussed EVBC control circuit, which limits active power demand for higher than nominal input ac voltages. The fundamental reactive power characteristics of EVBC model will shift from an approximately constant impedance load type (i.e. with n_q=2 and Z_q=1) to a combination of constant power and constant current load type (i.e. with n_q~I_q~P_q~0.5), again when the input ac supply voltage magnitude is higher than 1pu. The only exception are Q_1-V results for pointed-top voltage waveform with magnitude higher than 1pu, which closely resemble a constant power load type (n_q=0 and P_q=1). Measurement data in Fig. 13 confirm these active/reactive power characteristics, although most of measurements were done with the supply voltage magnitudes in the range 0.9pu-1.1pu, in order to prevent disconnection of tested EVBCs due to over or under voltage supply conditions.

V. CONCLUSIONS

This paper presents a component-based methodology for modelling on-board unidirectional single-phase electric vehicle battery chargers (EVBCs), typically used in domestic "slow-charging" applications. The modelling methodology begins with a detailed representation of the main EVBC circuit components, including full implementation of control algorithms and high frequency switching circuits. The model also includes representation of the EV battery (typically Li-ion type), in which the battery resistance is determined from the measurements and expressed as a function of the battery state of charge and input rms ac voltage.

In order to reduce the computational requirements and simulation times, the full circuit model is afterwards reduced to an equivalent circuit model form, by formulating an analytical expression for the equivalent dc-link resistance. Both full and equivalent circuit EVBC models were validated by measurements, demonstrating that they can accurately reproduce the most important electrical characteristics of EVBCs for a number of supply voltage conditions (ideally sinusoidal and distorted voltage waveforms, with different magnitudes). These results, based on a direct comparison of measurements of actual EVs and circuit simulations, confirm that the presented EVBC models are capable of correctly representing EVBCs in power system studies, including analysis of their harmonic emissions for power quality assessment.

The paper also discussed the use of the developed EVBC models for assessing the impact of increasing EVBC penetration levels on power flows and performance of LV and MV networks. For that purpose, exponential and polynomial/ZIP model interpretations are formulated, in order to specify and implement appropriate EVBC steady state load models for a large area network studies.

The dependency of EVBC characteristics on supply voltage distortions clearly indicates that the correct modelling of EVBCs should include a-PFC circuit and raises important questions about the suitability of compliance verification tests in [8], which require sinusoidal voltages for testing loads with a-PFC circuit. This is one of the possible directions for future work, together with the further development and specification of simple and accurate aggregate models of a large number of EVBCs, aimed at the analysis of existing LV and MV networks and future "smart grids".

REFERENCES

[1] K. Qian, C. Zhou, M. Allan, and Y. Yuan, "Modelling of load demand due to EV battery charging in distribution systems," *IEEE Trans. Power Systems*, vol. 26, no. 2, pp. 802-810, May 2011.

[2] L. Kutt, E. Saarijarvi, M. Lehtonen, H. Molder and J. Niitsoo, "Current harmonics of EV chargers and effects of diversity to charging load current distortions in distribution networks," *in Proc. 2013 Int. Conf. on Connected Vehicles and Expo (ICCVE)*, Las Vegas, NV, US, Dec. 2013, pp.726-731.

[3] M. Yilmaz and P. T. Krein, "Review of battery charger topologies, charging power levels, and infrastructure for plug-in electric and hybrid vehicles," *IEEE Trans. Power Electronics*, vol. 28, no. 5, pp. 2151-2169, May 2013.

[4] L. Wang, J. Liang, G. Xu, K. Xu and Z. Song, "A novel battery charger for plug-in hybrid electric vehicles," *in Proc. 2012 Int. Conf. on Information and Automation (ICIA)*, Shenyang, China, Jun. 2012, pp. 168-173.

[5] E. Abdelhamid; A. K. Abdelsalam; A. Massoud and S. Ahmed, "An enhanced performance IPT based battery charger for electric vehicles application," *in Proc. IEEE 23rd Int. Symposium on Industrial Electronics (ISIE)*, Istanbul, Turkey, Jun. 2014, pp. 1610-1615.

[6] A. Collin, S. Djokic, H. Thomas and J. Meyer, "Modelling of electric vehicle chargers for power system analysis," *in Proc. 11th Int. Conf. on Electric Power Quality and Utilisation*, Lisbon, Portugal, Oct. 2011.

[7] IEC BS/EN, "*Electric vehicle conductive charging system. Part 21: Electric vehicle requirements for conductive connection to an ac/dc supply*", IEC Standard 61851-21, 2002.

[8] IEC BS/EN, *Electromagnetic compatibility (EMC) — Part 3-2: Limits for harmonic current emissions (equipment input current ≤ 16 A per phase)*, IEC Standard 61000-3-2, 2009.

[9] S. Müller, F. Möller, J. Meyer, A. J. Collin and S. Z. Djokic, "Characterisation of harmonic interactions between electric vehicle battery chargers and PV inverters", *in Proc. IEEE Int.Conf. on Harmonics and Quality of Power*, Bucharest, Romania, May 2014.

[10] B. Singh, B. N. Singh, A. Chandra, K. Al-Haddad, A. Pandey, and D.P. Kothari, "A review of single-phase improved power quality AC–DC converters," *IEEE Trans. Ind. Elect*., vol. 50, no. 5,pp.962–981, Oct. 2003.

[11] *IEEE standard definitions for the measurement of electric power quantities under sinusoidal, non-sinusoidal, balanced, or unbalanced conditions, IEEE Std 1459-2010*.

[12] A. J. Collin, I. Hernando-Gil, J. L. Acosta and S. Z. Djokic, "An 11 kV steady state residential aggregate load model," in *Proc. IEEE PES PowerTech Conf.*, Trondheim, Norway, Jun. 2011.